

Visible light driven amide synthesis in water at room temperature from Thioacid and amine using CdS nanoparticles as heterogeneous Photocatalyst

Sudipto Das | Shounak Ray | Abhisek Brata Ghosh | Partha Kumar Samanta |

Suvendu Samanta | Bibhutoh Adhikary | Papu Biswas 

Department of Chemistry, Indian Institute of Engineering Science and Technology, Shibpur, Howrah 711 103, West Bengal, India

Correspondence

Papu Biswas, Department of Chemistry, Indian Institute of Engineering Science and Technology, Shibpur, Howrah 711 103, West Bengal, India.

Email: papubiswas_besus@yahoo.com; pb.besu.chem@gmail.com

Highly efficient photocatalytic thioacid mediated amide synthesis at room temperature using CdS nanoparticles as photocatalyst was observed under a household 30 W CFL in water. The operationally mild reaction was tolerant to a number of functional group substitutions on amine and could be scaled up to gram. This heterogeneous photocatalyst was extremely stable and could easily be recovered by simple centrifugation for at least six recycling reactions without any significant loss of catalytic performance. The possible reaction mechanism for the photocatalytic thioacid mediated amide synthesis over the CdS semiconductor has also been proposed on the basis of experimental observations.

KEYWORDS

amide synthesis, aqueous medium, CdS nanoparticles, heterogeneous catalyst, thioacids

1 | INTRODUCTION

Visible light driven photoredox processes at ambient temperature have emerged as a powerful synthetic tool to develop sustainable synthetic routes. Polypyridine complexes of ruthenium and iridium are generally employed as efficient visible light photocatalysts in most of these reactions.^[1] Few organic dyes have also been successfully utilized as visible light photoredox catalysts.^[2] However, these homogeneous catalytic processes suffered from a serious limitation, namely, the separation and recovery of the catalyst. Therefore, heterogeneous semiconductor visible light photoredox catalysis is emerging to provide radically new synthetic applications. In particular, CdS is widely regarded as an excellent visible light-driven photocatalyst. CdS is one of the most attractive II–VI semiconductors with a direct bulk phase band gap (2.4 eV). Due to its narrow band gap and favorable band structure CdS has been extensively studied for visible light photocatalytic H₂ evolution^[3–5] and organic dye degradation. Though CdS is widely regarded as an excellent visible

light-driven photocatalyst, the efficiency of pure CdS nanoparticles are not satisfactory as photocatalyst in fine chemical synthesis due to the recombination of the photo-generated electron–holes and the photocorrosion ($\text{CdS} + \text{h}^+ \rightarrow \text{Cd}^{2+} + \text{S}$).^[6] There have been considerable efforts to overcome the problem and many nanocomposites such as TiO_2/CdS ,^[7] $\text{TiO}_2/\text{graphene}/\text{CdS}$,^[8] CdS/rGO ,^[9] $\text{CdS}/\text{g-C}_3\text{N}_4$,^[10] and $\text{graphene}/\text{CdS}/\text{metal ion}$ (Ca^{2+} , Cr^{3+} , Mn^{2+} , Fe^{2+} , Co^{2+} , Ni^{2+} , Cu^{2+} and Zn^{2+})^[11] composite have been investigated as promising photocatalysts for visible light-driven organic transformations. To date, there are very few reports on photocatalytic activity of pure CdS nanoparticles in fine chemical synthesis.^[12]

Amide bonds are ubiquitous in numerous organic molecules, such as peptides, natural products, and pharmaceutical agents.^[13–15] Amides are also utilized as ligands and catalysts in organic synthesis, as well as amide bonds are the basis for some of the most versatile and widely used synthetic polymers.^[13–15] Currently, most widely used amide synthesis pathways rely on

activation of a carboxylic acid using an expensive and toxic coupling reagent such as a carbodiimide, uronium or phosphonium and subsequent coupling of the activated species with an amine.^[16] Although amide bond could be generated efficiently using coupling reagents, these methodologies suffer from the inherent drawback of producing stoichiometric amounts of unwanted co-products. Alternatively, several metallic,^[7,16b,c] organocatalyst and arylboronic acid^[16b] catalysts for the synthesis of amides have also been developed to circumvent this problem. Though most of these catalytic methods lead to higher efficiency and produce less organic waste, more environmentally benign protocol would likely be welcomed as most of these reactions are done in organic solvents and at high temperature. Hence, issues such as catalytic recyclability, waste disposal, safety, reaction at room temperature and utilization of greener solvent (e.g. water) need further attention. So far, only few methodologies have been developed which exploit greener solvents, such as water, as the reaction medium for amide bond synthesis.^[17]

Recently, the thioacid mediated amide bond formation has attracted much attention due to their unique reactivity and selectivity compared to those of carboxylic acids. The reactivity of thioacids with organo-azides,^[18] isonitriles,^[19] -thioisocyanates,^[20] -isocyanates,^[20] -aziridines,^[21] electron deficient sulphonamides,^[22] nitroso derivatives,^[23] and dinitrofluorobenzene^[24] have been efficiently exploited in the direct peptide bond formation or native chemical ligation. These methodologies require expensive substrates and suffer from limited substrates scope. Further, Xian and co-workers also demonstrated the synthesis of amide bonds from thioacids and amines via formation of S-nitrosothioacids (NTA) at 0 °C.^[23] Wu *et al.* reported^[25] the in situ activation of thioacids through the formation of silatropic switch with bistrimethylsilylacetamide (BSA) followed by the peptide bond formation. Recently, Mali *et al.* reported the copper sulfate mediated ultrafast peptide synthesis using N-protected thioacids and mild N-acylation of amines mediated by thioacids in methanol.^[26] Very recently, [Ru(bpy)₃]Cl₂ catalyzed visible-light-promoted methodology involving amines and potassium salt of thioacids have also been reported by Liu *et al.*^[27] Moreover, recent reports demonstrate visible light photocatalytic generation of thiyl radicals and their exploitation in organic transformation.^[28] We have earlier reported synthesis of spherical or quasi-spherical CdS nanoparticles and its photocatalytic activity in generation of 2-substituted benzothiazoles from various alkyl and aryl aldehydes under visible light irradiation.^[29] In view of the importance of thioacid mediated amide bond synthesis and inspired by the ability of visible light photocatalysts to

produce thiyl radicals, we report herein a simple, clean, recyclable and efficient photocatalytic method for the synthesis of amide bonds from thioacids and simple amines in water at room temperature by visible-light irradiation of CdS nanoparticles (CdSNPs).

2 | EXPERIMENTAL SECTION

2.1 | Materials and methods

All chemicals including bulk CdS and WO₃ were obtained from commercial sources and used as received without further purification. All solvents were analytical grade and distilled before use. CdS nanoparticles (CdSNPs) were synthesized following the method reported by us earlier.^[29] Thin layer chromatography (TLC) was performed on EMD pre-coated plates silica gel (60 F254, 0.25 mm thickness) and visualized by fluorescence quenching under UV light. Column chromatography was performed on Silica Gel (60–120 Mesh).

2.2 | Physical measurements

Powder X-ray diffraction (XRD) patterns were obtained on a Philips PW 1140 parallel beam X-ray diffractometer with Bragg-Bretano focusing geometry and monochromatic CuK α radiation ($\lambda = 1.540598$ Å). Transmission Electron Microscopy (TEM) imaging was done on a Philips FEI CM 200 transmission electron microscope operated at 200 kV. TEM samples were prepared by sonicated an aliquot of the sample in ethanol for 15 min and a single drop (2 μ L) of this suspension was drop-casted onto carbon-coated, 300 mesh copper grids. Grids were allowed to air dry prior to imaging. Absorption spectra were carried out on an Agilent 8453 diode array spectrophotometer. ¹H NMR spectra were recorded on a Bruker Avance III 400 and 500 MHz NMR spectrometer. N₂-sorption isotherms were obtained using a Quantachrome Instruments analyzer at 77 K. LC-MS was obtained from Agilent Quadrapole LC-MS 6120 Series. GC analyses were performed on an Agilent Technologies 6890 N network GC system with an FID detector using a J & W HP-5 column (30 m, 0.32 mm internal diameter), nitrogen as carrier gas and n-decane as the internal standard.

2.3 | Photoelectrochemical measurements

All the electrochemical experiments were performed with a CHI-660E electrochemical workstation (CHI Instruments, USA). The working electrode for photo electrochemical measurement has been fabricated by the drop-casting method reported by Wang and his group.^[30] Initially, the ITO coated glass slide was washed carefully

using water-acetone-isopropanol. Then the conducting side of the glass slide was drop coated with a concentrated solution of CdS nanoparticles and dried under an inert atmosphere at 100 °C for 10–15 min. Approximately, five to six layers of CdS solution were drop coated onto the device following the same procedure. The film was then annealed at 200 °C for 1 h to use it as a working electrode. The photoelectrochemical measurements were conducted in a typical three-electrode configuration where Ag/AgCl is used as a reference and Pt as a counter electrode and 0.1 M Na₂SO₄ solution as the electrolyte (pH 7). The photovoltaic characteristics and photo current response was measured using linear sweep voltammetry within a potential range -0.5 to 0.5 V at a scan rate of 0.1 Vs⁻¹ using a 300 W Xe lamp. The photo sensitivity of the materials was investigated by measuring the current in dark and under illumination chronoamperometrically by light on-off cycle at a steady voltage of 0.5 V vs Ag/AgCl in 10 s intervals. The potential versus RHE was calculated with reference to Ag/AgCl following the Nernst equation:

$$E_{\text{RHE}} = E_{\text{Ag/AgCl}} + E_0 + 0.059\text{pH}$$

where E_{RHE} is the potential vs RHE, $E_{\text{Ag/AgCl}}$ is the measured potential vs Ag/AgCl and $E_0 = 0.2$ V at 25 °C.

EIS were performed under illumination in the same electrode cell containing 5 mM K₃Fe(CN)₆/K₄Fe(CN)₆ (1:1) and 0.1 M KCl. The impedance measurements were recorded at open-circuit potential (OCP) within the frequencies ranged from 100 kHz to 1 Hz using a sinusoidal perturbation potential of 100 mV.

2.4 | Catalytic reactions and product analyses

In a 25 ml round bottom flask, 4 mg CdSNPs were dispersed in 10 ml water and sonicated for 15 minutes. Thioacid (2 mmol) and amine (2 mmol) were added to the CdSNPs dispersed solution. The mixed solution was then irradiated with a 30 watt household CFL at a distance of 4 cm in a closed box. The progress of the reaction was monitored by TLC or gas chromatography. After the completion of reaction, the catalyst was separated by centrifugation and washed with ethanol (4×5 ml), dried in air and reused. Then reaction mixture was evaporated at reduced pressure and the product was dissolved in minimum volume of dichloromethane (DCM). The solution was washed with water (3×5 ml) and the DCM layer was dried over anhydrous Na₂SO₄. Product was then purified by column chromatography using silica gel to

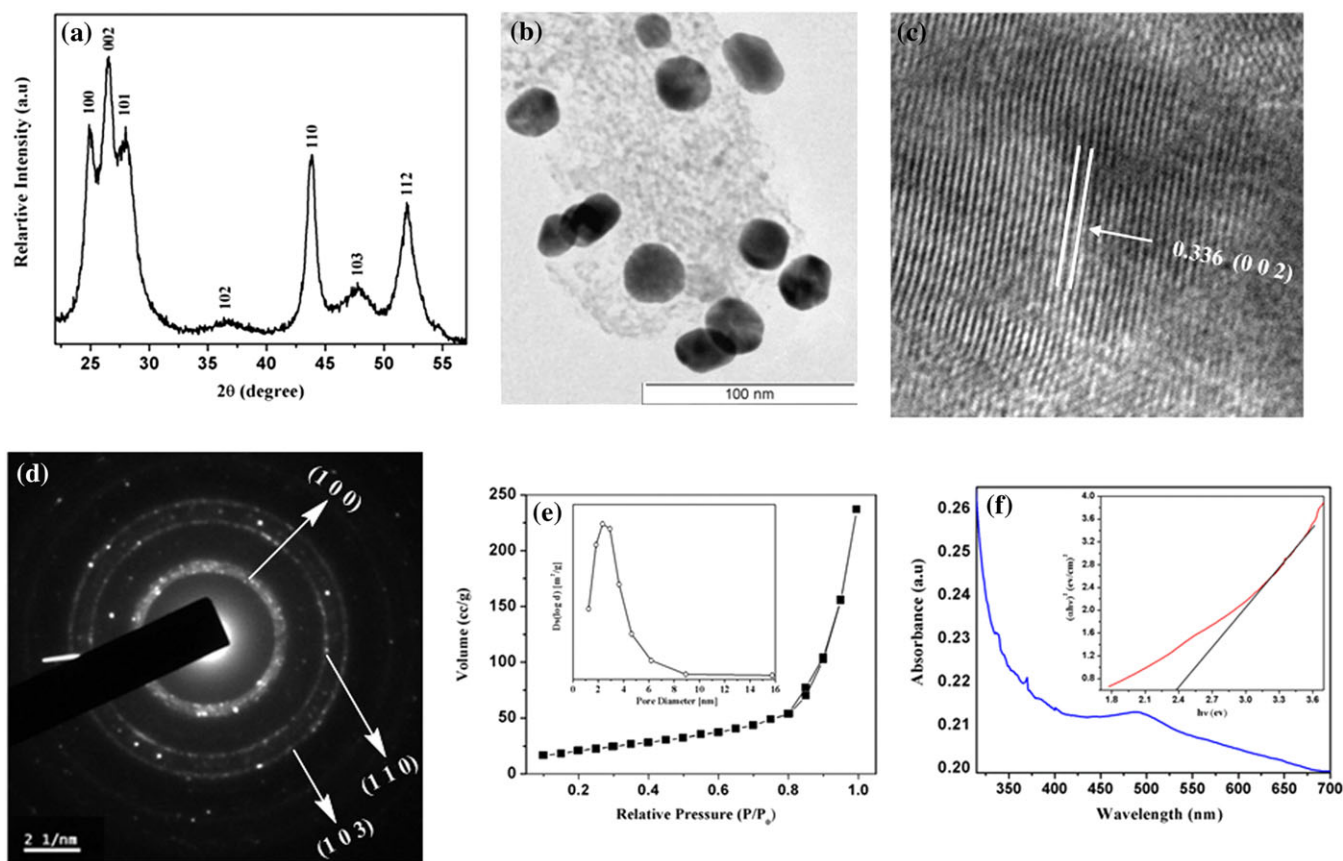


FIGURE 1 (a) PXRD, (b) TEM, (c) HR-TEM, (d) SAED pattern, (e) BET and (f) UV-Vis spectrum and band gap energies (inset) in water of the synthesized CdSNPs catalyst

get desired product. Reported yields are the average of at least three runs.

3 | RESULTS AND DISCUSSION

3.1 | Structural and photoelectrochemical characterization of CdSNPs

The CdSNPs were synthesized as previously described by us^[29] and characterized by powder XRD and transmission electron microscope (TEM). The well resolved X-ray diffraction peaks (Figure 1a) of the synthesized CdSNPs can be indexed to the hexagonal structure of CdS (JCPDS card No. 41-1049). The synthesized CdSNPs are composed of spherical or quasi-spherical nanoparticles (Figure 1b) with average diameter of 20–25 nm as observed earlier by us.^[29] From the HRTEM image of CdSNPs (Figure 1c), it is obvious that the surface in an individual CdNP is single crystalline with a lattice fringe spacing of 0.336 nm corresponding to the (002) plane. Selected area electron diffraction (SAED) patterns of CdSNPs (Figure 1d) exhibits concentric rings that can be indexed to (100), (110) and (103) diffraction planes for hexagonal CdS. The X-ray diffraction peaks (Figure S1a) of the commercial CdS can be indexed to the hexagonal structure of CdS (JCPDS card No. 41-1049). Diffraction peaks (Figure S1b) of the commercial WO₃ correspond to the monoclinic phase of WO₃ (JCPDS 43-1035). These results are consistent with the observations made from the XRD patterns. The BET (Brunauer–Emmett–Teller) surface area of the CdSNPs was found to be 16.7 m² gm⁻¹ (Figure 1e). The BET surface area of the commercial CdS and WO₃ were found to be 2.3 and 8.5 m² gm⁻¹, respectively (Figure S2). It can be seen that the CdSNPs demonstrate high photo-absorption capacity in visible light around 520 nm in water (Figure 1f), suggesting its potential photocatalytic activity under visible light. The direct band gap energy (E_g) of the CdSNPs was estimated from the $(\alpha h\nu)^{1/2}$ versus photon energy ($h\nu$) plot (inset of Figure 1f) and calculated to be 2.39 eV.

To understand and investigate the origin of the good photocatalytic activity of CdSNPs, a series of characterizations have been carried out. The electrochemical impedance characteristic of CdSNPs was studied to understand the charge transfer behaviour which also governs the redox activity of the material. Figure 2a represents the typical Nyquist plot of CdSNPs where the characteristic semicircle is indicative of a single charge transfer process taking place between working electrode and the electrolyte solution. In a Nyquist plot, the diameter of the semicircle, which is basically the measure of the charge transfer resistance (R_{CT}) of the respective electrode interface, is an important factor for the consideration of the

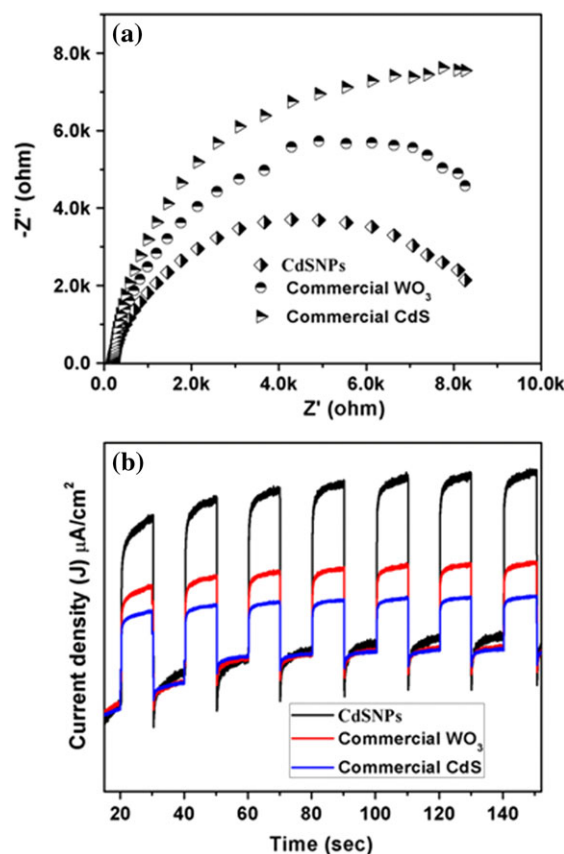


FIGURE 2 (a) Nyquist impedance plot of the heterogeneous catalysts in 0.1 M KCl aqueous solution containing 5 mM K₃Fe(CN)₆–K₄Fe(CN)₆, (b) Current density versus time plot during successive on and off cycles of light of the heterogeneous catalysts in a 0.1 M Na₂SO₄ aqueous solution

electrode kinetics and the electron transfer behaviour of the material. In the present case the value of R_{CT} is calculated as 9.4 K Ω . As presented in Figure 2a, the impedance radius of CdSNPs was smaller than that of commercial CdS and WO₃. Generally, a smaller arc radius on EIS (Nyquist plots) represents a faster interfacial charge transfer and higher separation efficiency of photogenerated charge carriers. The results therefore demonstrated that CdSNPs more favorably transferred and separated photogenerated charge carriers than the commercial CdS and WO₃. Figure S3a exhibits the current density (J) versus voltage plot of CdSNPs nanostructure in dark and under light. As evident from the study, the current density under light is significantly higher than that of dark and the corresponding photocurrent gain ($J_{\text{light}}/J_{\text{dark}}$) is estimated as 2.6. To investigate the photostability of the material the current density versus time measurement has been carried out by consecutive light on and off mode at 10 s intervals at a constant potential (0.5 V vs Ag/AgCl). The study reveals that the material has sufficient stability with no loss of current density over a period of 150 s (Figure 2b). It is also clear that the

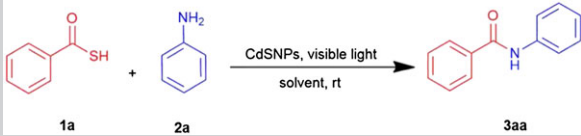
photocurrent response of CdSNPs was significantly higher than that of commercial CdS and WO₃ under the same visible-light illumination (Figure 2).

3.2 | Catalytic reaction

In continuation to our effort to evaluate the visible light-driven photocatalytic activity of pure CdS nanoparticles in synthesis of fine chemicals,^[29] we decided to investigate the thioacid mediated amide bond formation with amine in water. The reaction between thiobenzoic acid **1a** and aniline **2a** was conducted as a model reaction over the CdSNPs to optimize the reaction conditions (solvent, time and catalyst loading), and the results are summarized in Table 1. As evident from Table 1, water was the optimal solvent, while other commonly used solvents

such as chloroform (CHCl₃), dichloromethane (DCM), ethanol (EtOH), methanol (MeOH), acetonitrile (MeCN) and tetrahydrofuran (THF) gave inferior yields (entries 1–7). We then screened a variety of commonly used and commercially available heterogeneous photocatalysts such as CdS, WO₃ and TiO₂ P25. It turned out that CdSNPs was the best catalyst among all the heterogeneous photocatalysts tested (entries 8–10). We have also examined efficacy of CuSO₄·5H₂O as catalyst in water in absence of visible light^[26] and found to give much inferior yield (entry 11). Then we have tested two well-known homogeneous catalysts, Ru(bpy)₃Cl₂ and rose bengal (entries 12,13). Both catalysts were found to furnish inferior yield in water than CdSNPs. In order to evaluate the ideal catalyst amount, the reactions were performed using 2–10 mg of CdSNPs (entries 5 and 14–17). The optimum reaction conditions are 3 hr and in presence of 4 mg

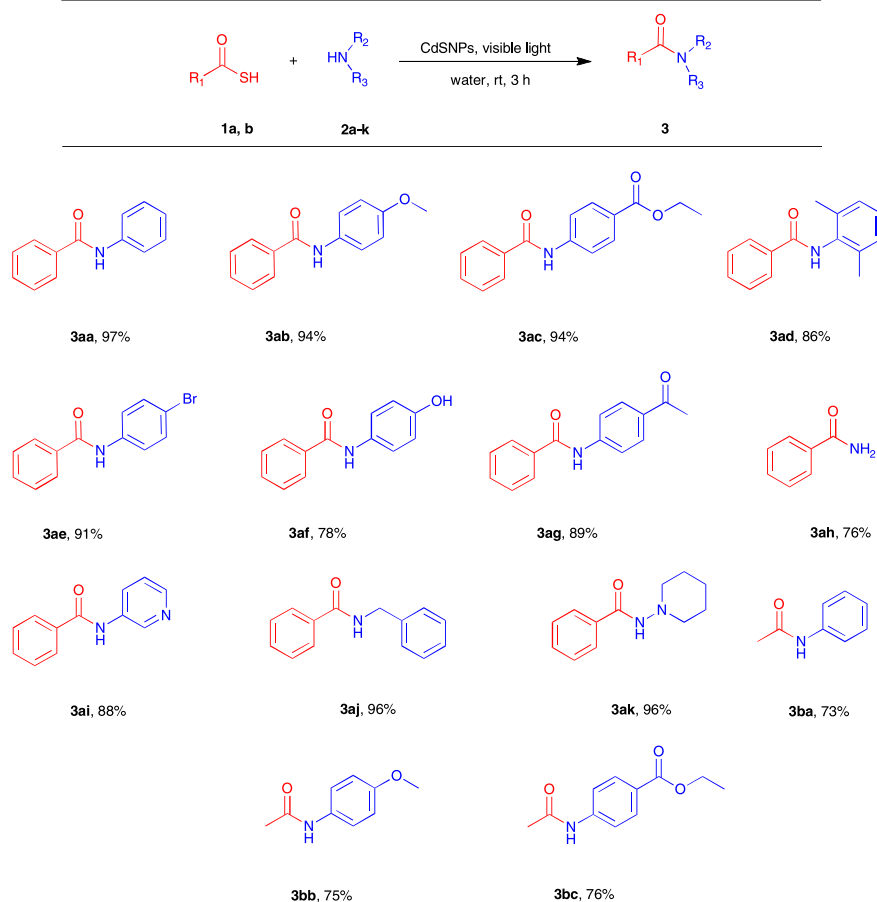
TABLE 1 Optimization of the reaction conditions^a

					
Entry	Solvent	Catalyst	Time (h)	Amount of cat. (mg)	Yield (%) ^b
1	CHCl ₃	CdSNPs	5.0	10	69
2	DCM	CdSNPs	5.0	10	72
3	MeOH	CdSNPs	5.0	10	85
4	EtOH	CdSNPs	5.0	10	81
5	H ₂ O	CdSNPs	5.0	10	98
6	MeCN	CdSNPs	5.0	10	53
7	THF	CdSNPs	5.0	10	60
8	H ₂ O	CdS (bulk)	5.0	10	31
9	H ₂ O	WO ₃ (bulk)	5.0	10	23
10	H ₂ O	TiO ₂ P25	5.0	10	Trace
11 ^c	H ₂ O	CuSO ₄ ·5H ₂ O	5.0	150	63
12	H ₂ O	Ru(bpy) ₃ Cl ₂	5.0	10	47
13	H ₂ O	Rose Bengal	5.0	10	34
14	H ₂ O	CdSNPs	5.0	8	98
15	H ₂ O	CdSNPs	5.0	6	97
16	H ₂ O	CdSNPs	5.0	4	97
17	H ₂ O	CdSNPs	5.0	2	68
18	H ₂ O	CdSNPs	4.0	4	98
19	H ₂ O	CdSNPs	3.0	4	97
20	H ₂ O	CdSNPs	2.0	4	83

^aReaction conditions: **1a** (2.0 mmol), **2a** (2.0 mmol), catalyst in solvent (10 ml), room temperature.

^bIsolated yield.

^cReaction carried out in absence of visible light using 30 mol% of catalyst.



SCHEME 1 Substrates scope in amide bond formation. Reaction conditions: **1** (2.0 mmol), **2** (2.0 mmol), catalyst (4 mg), water (10 ml), room temperature, visible light, 3 h. Isolated yields are reported

catalyst in water. Further prolonging the reaction time or increasing the amount of catalyst did not improve the yield of the reaction.

With optimized reaction conditions in hand, we next examined the substrate scope and versatility of this methodology. As shown in Scheme 1, a wide range of aromatic aniline derivatives **2** upon reaction with thiobenzoic acid **1a** afforded corresponding products **3aa–3ag** with the yield ranging from 97% to 78%. The results indicated that aniline, substituted anilines with electron-donating group (-OMe and -OH), electron withdrawing group (-COOEt and CHO) at *para*-positions, electronically neutral group (-CH₃) at *ortho* position, and halogen group (-Br) at *para*-position smoothly transformed into the desired products in good to excellent yields (Scheme 1). To further extend the utility of this methodology, ammonia **2h**, 3-amino pyridine **2i**, benzyl amine **2j** and piperidine **2k** were employed to react with thiobenzoic acid **1a** under

the optimized reaction conditions, all effectively affording the corresponding amide products **3ah–3ak** in moderate to excellent yields (76%–96%, Scheme 1). Steric effects had a little influence on the reaction since 2,6-dimethylaniline and piperidine gave excellent yields (Scheme 1, **3ad** and **3ak**). Next we examined reactivity of thioacetic acid **1b** with aromatic anilines (Scheme 2). Thioacetic acid was found to react smoothly with aniline amines **2a–2c** under optimal conditions to provide the corresponding amide products **3ba–3bc** in very good yields (Scheme 1, 73–76%).

Subsequently, we explored how the reaction performed in sunlight compared with the visible light source. Results demonstrate that with a natural illuminance of 44 000 lx (January, 22.555° N, 88.307° E, 12 m above sea level), over 90% conversion to **3aa** was observed in just 3 h. These conditions allow a fast and highly efficient synthesis of thioacid mediated amide bond, even in relatively moderate sunlight.

To demonstrate the synthetic applicability of this reaction, a gram scale reaction was performed under standard conditions with thiobenzoic acid and aniline. The desired N-phenylbenzamide **3aa** was obtained in 88% yield (Scheme 2).

An important feature of any heterogeneous catalytic system is their ability of reusability. Thus, recyclability



SCHEME 2 A gram-scale preparation of N-phenylbenzamide **3aa**

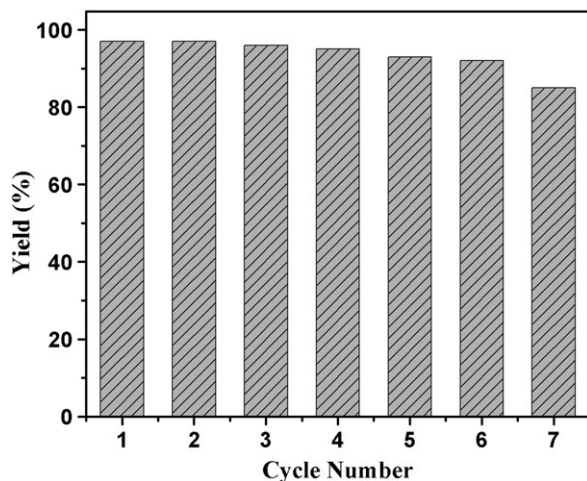


FIGURE 3 Recyclability test for the CdSNPs in the thioacid mediated amide bond formation

test for this catalytic system was evaluated. The catalyst after every run was recovered by simple centrifugation and followed by washing with ethanol. The substrates thiobenzoic acid **1a** and aniline **2a** were employed in these experiments. The catalyst could be recycled at least 6 times without any significant loss of catalytic performance (Figure 3). The experimental results demonstrate that the performance of CdSNPs shows some minor degradation after six times reuse. To understand deactivation, after the sixth run, the spent catalyst was characterized by TEM and BET (Figure 4). Figure 4a demonstrates that the morphology of the CdSNPs appear not to be modified but agglomeration of CdSNPs observed by action of the chemical reaction. This is consistent with lower specific surface area ($9.04 \text{ m}^2 \text{ g}^{-1}$) found in BET (Figure 4b). X-Ray diffraction (XRD) pattern (Figure 4c) indicates that the crystal structure of the CdS photocatalyst is intact after the reaction though diffraction peaks due to (100), (101) and (102) are not well resolved due to agglomeration.

3.3 | Mechanistic studies

In order to verify the feasibility of the photocatalytic activity by CdSNPs, the band position of the as-prepared CdSNPs photocatalyst was evaluated by Mott–Schottky plot. It was found that the slope of the linear $1/C^2$ potential curve was positive, indicating that CdS has an n-type semiconductor characteristic (Figure S3b).^[31,32] The flat-band potential (V_{fb}) of CdSNPs was determined from extrapolation to the X intercept in the Mott–Schottky plot at various frequencies. V_{fb} of CdS is approximately -1.001 V vs. Ag/AgCl. Therefore, the conduction band (CB) and valence band (VB) positions are found to be -0.804 V and 1.586 V , respectively (Figure 5).

To obtain more insight of the reaction mechanism, a series of additional experiments were conducted (Scheme 3). The reaction between thiobenzoic acid **1a** and aniline **2a** in absence of CdSNPs or visible light led to the formation of amide **3aa** in trace amounts under the optimized reaction conditions. Thiobenzoic acid **1a** in absence of amine upon irradiation under visible light in presence of CdSNPs provided corresponding disulfide **4**. Subsequently, treatment of the freshly prepared disulfide **4** with aniline **2a** effectively afforded the corresponding amide product **3aa**.

On the basis of the control experiments and previous reports,^[27,33] a plausible mechanism is proposed, as shown in Figure 5. First, thioacid **1** in presence of CdSNPs photocatalyst reacts with hole generated under visible light illumination and produce disulfide intermediate **4**. In aqueous solution the acetyl/benzoyl thiolates generated from thioacids coordinated with Cd(II) ions at the surface of CdSNPs.^[34] The hole transfer from the excited CdSNPs to bound thiolates occurs easily to generate surface-bound acetyl/benzoyl thiyl radicals. The feasibility of formation of the acetyl/benzoyl thiyl radicals can be verified from the positions of the conduction band and

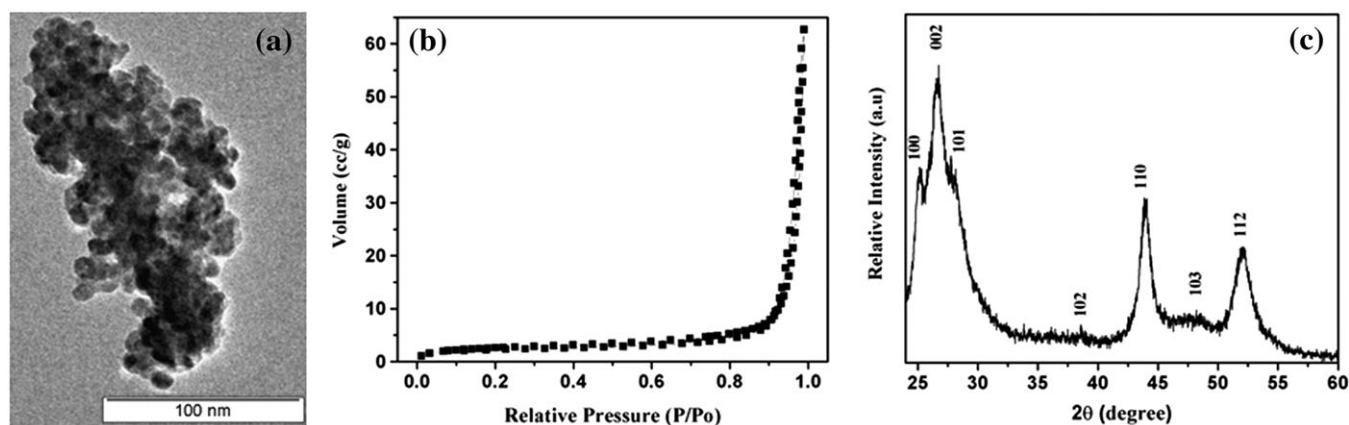


FIGURE 4 (a) TEM (b) BET, and (c) PXRD of the reused CdSNPs catalyst for the thioacid mediated amide bond synthesis after the sixth run

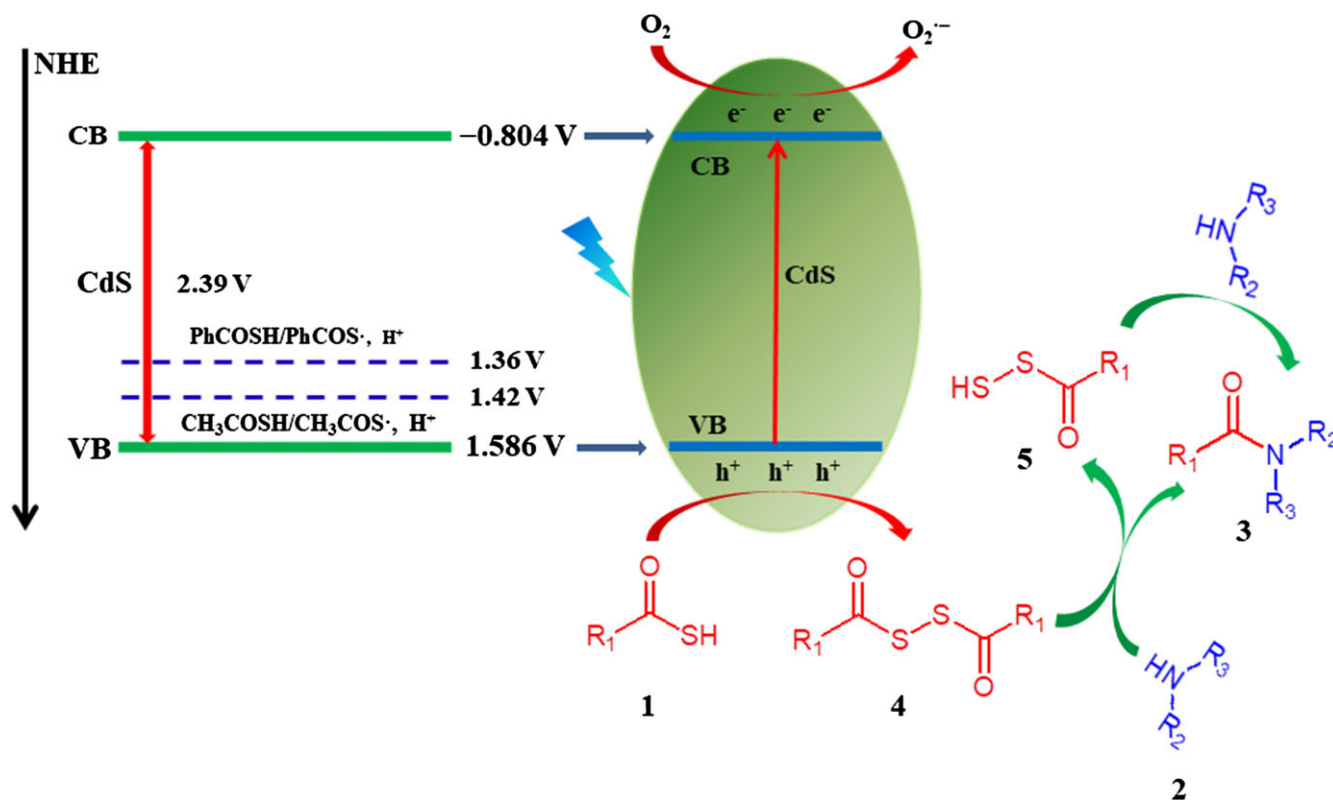


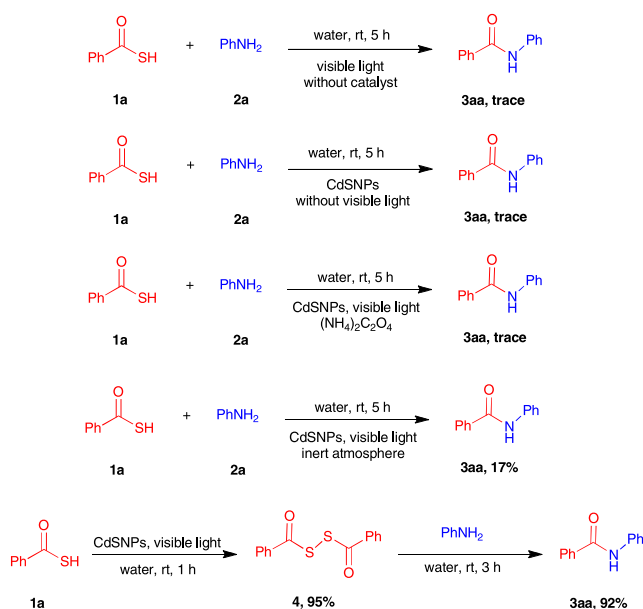
FIGURE 5 Band positions of CdSNPs, redox potentials of thioacids and proposed reaction mechanism

valence band of CdSNPs and the redox potential of $\text{PhCOS}^\bullet, \text{H}^+/\text{PhCOSH}$ and $\text{CH}_3\text{COS}^\bullet, \text{H}^+/\text{CH}_3\text{COSH}$,^[35,36] which reveals that the valence band of CdSNPs is more positive than the oxidative potential (Figure 5) of $\text{PhCOSH}/\text{PhCOS}^\bullet, \text{H}^+$ ($E^\circ_{\text{PhCOSH}/\text{PhCOS}^\bullet, \text{H}^+} = 1.36 \text{ V vs. NHE}$) and $\text{CH}_3\text{COSH}/\text{CH}_3\text{COS}^\bullet, \text{H}^+$ ($E^\circ_{\text{MeCOSH}/\text{MeCOS}^\bullet, \text{H}^+} = 1.42 \text{ V vs. NHE}$). Therefore, a green photocatalytic

process for oxidation of RCOSH to $\text{RCOS}^\bullet, \text{H}^+$ could be achieved. Alkyl/arylthiyl radicals readily form disulfide. To prove participation of the hole generated, reaction was carried out in presence of hole scavenger ammonium oxalate ($(\text{NH}_4)_2\text{C}_2\text{O}_4$). No product obtained when reactions were carried out in presence of hole scavenger. In-situ generated disulfide then simultaneously converted into amide in presence of amine. The intermediate **5** could further produce amide through aminolysis as reported previously.^[33] Aerobic oxygen probably plays a crucial role to complete the photoredox cycle by accepting electron from conduction band to form superoxide radical anion $\text{O}_2^{\bullet-}$ as $E^\circ(\text{O}_2/\text{O}_2^{\bullet-}) = -0.16 \text{ V}$.^[37] To confirm the involvement of aerobic oxygen, a control experiment (Scheme 2) under inert atmosphere was performed and found to furnish much inferior yield (17%).

4 | CONCLUSION

The CdS photocatalyst showed excellent photocatalytic activity for the thioacid mediated amide synthesis with amine in water under visible light irradiation, giving 73–97% yields of amides. Several functional groups were well tolerated under the reaction conditions employed, such as methoxy, ester, bromide, aldehyde and phenolic –OH. Most significantly, the methodology developed was



SCHEME 3 Control experiments

simple, easily handled and the reactions were performed in water. Furthermore, the procedure can be performed effectively using a visible light source or alternatively even in relatively moderate sunlight. Recyclability test of the reaction mixture showed that CdS photocatalyst maintain their excellent catalytic activity even after six reused cycle. The excellent photocatalytic activity of CdS is attributed to its well placed conduction band and valance band positions, efficient visible light absorption and highly effective separation of photogenerated charge carriers. The results of the present work are of greatly significant in practice and useful in the exploitation of clean and safe solar energy.

ACKNOWLEDGMENTS

SR thanks IEST, Shibpur for Institute Research Fellowship and PKS acknowledges UGC-India for JRF (ID-131818). We acknowledge SAIF-NEHU for providing NMR facility.

ORCID

Papu Biswas  <http://orcid.org/0000-0002-7697-849X>

REFERENCES

- [1] For leading references on visible-light photoredox catalysis, see: a) C. K. Prier, D. A. Rankic, D. W. C. MacMillan, *Chem. Rev.* **2013**, *113*, 5322. b) J. M. R. Narayanam, C. R. J. Stephenson, *Chem. Soc. Rev.* **2011**, *40*, 102. c) J. W. Tucker, C. R. J. Stephenson, *J. Org. Chem.* **2012**, *77*, 1617. d) T. P. Yoon, M. A. Ischay, J. Du, *Nat. Chem.* **2010**, *2*, 527 and references therein.
- [2] a) J. H. Park, K. C. Ko, E. Kim, N. Park, J. H. Ko, D. H. Ryu, T. K. Ahn, J. Y. Lee, S. U. Son, *Org. Lett.* **2012**, *14*, 5502. b) S. Samanta, S. Das, P. Biswas, *J. Org. Chem.* **2013**, *78*, 11184. c) X. Gu, X. Li, Y. Chai, Q. Yang, P. Li, Y. Yao, *Green Chem.* **2013**, *15*, 357. d) J. Luo, X. Zhang, J. Zhang, *ACS Catal.* **2015**, *5*, 2250. e) X. Wu, C. Meng, X. Yuan, X. Jia, X. Qian, J. Ye, *Chem. Commun.* **2015**, *51*, 11864. f) D. A. Nicewicz, T. M. Nguyen, *ACS Catal.* **2014**, *4*, 355. g) D. Ravelli, M. Fagnoni, *Chem. Cat. Chem.* **2012**, *4*, 169. h) C. Vila, J. Lau, M. Rueping, *Beilstein J. Org. Chem.* **2014**, *10*, 1233. i) J. Li, H. Wang, L. Liu, J. Sun, *RSC Adv.* **2014**, *4*, 49974. j) S. Fukuzumi, K. Ohkubo, *Org. Biomol. Chem.* **2014**, *12*, 6059.
- [3] a) Y. Xu, W. Zhao, R. Xu, Y. Shi, B. Zhang, *Chem. Commun.* **2013**, *49*, 9803. b) Q. Li, X. Li, S. Wageh, A. A. Al-Ghamdi, J. Yu, *Adv. Energy Mater.* **2015**, *5*, 1500010. c) J. Yuan, J. Wen, Q. Gao, S. Chen, J. Li, X. Li, Y. Fang, *Dalton Trans.* **2015**, *44*, 1680. d) J. Yuan, J. Wen, Y. Zhong, X. Li, Y. Fang, S. Zhang, W. Liu, *J. Mater. Chem. A* **2015**, *3*, 18244. e) S. Ma, J. Xie, J. Wen, K. He, X. Li, W. Liu, X. Zhang, *Appl. Surf. Sci.* **2017**, *391*, 580. f) T. Di, B. Zhu, J. Zhang, B. Cheng, J. Yu, *Appl. Surf. Sci.* **2016**, *389*, 775. g) D. Zhao, Q. Wu, C. Yang, R. T. Koodali, *Appl. Surf. Sci.* **2015**, *356*, 308. h) J.-J. Zhou, R. Wang, X.-L. Liu, F.-M. Peng, C.-H. Li, F. Teng, Y.-P. Yuan, *Appl. Surf. Sci.* **2015**, *346*, 278. i) J. Ran, J. Yu, M. Jaroniec, *Green Chem.* **2011**, *13*, 2708. j) Q. Wang, J. Li, Y. Bai, J. Lian, H. Huang, Z. Li, Z. Lei, W. Shangguan, *Green Chem.* **2014**, *16*, 2728. k) S. K. Apte, S. N. Garaje, M. Valant, B. B. Kale, *Green Chem.* **2012**, *14*, 1455. l) M.-Q. Yang, Y.-J. Xu, *Phys. Chem. Chem. Phys.* **2013**, *15*, 19102. m) N. Zhang, M.-Q. Yang, S. Liu, Y. Sun, Y.-J. Xu, *Chem. Rev.* **2015**, *115*, 10307.
- [4] S. R. Lingampalli, U. K. Gautam, C. N. R. Rao, *Energy Environ. Sci.* **2013**, *6*, 3589.
- [5] L. Shang, B. Tong, H. Yu, G. I. N. Waterhouse, C. Zhou, Y. Zhao, M. Tahir, L.-Z. Wu, C.-H. Tung, T. Zhang, *Adv. Energy Mater.* **2016**, *6*, 150241.
- [6] a) J. Yang, D. Wang, H. Han, C. Li, *Acc. Chem. Res.* **2013**, *46*, 1900. b) A. Kudo, Y. Miseki, *Chem. Soc. Rev.* **2009**, *38*, 253.
- [7] N. Qin, Y. Liu, W. Wu, L. Shen, X. Chen, Z. Li, L. Wu, *Langmuir* **2015**, *31*, 1203.
- [8] M. Q. Yang, Y. Zhang, N. Zhang, Z.-R. Tang, Y. J. Xu, *Sci. Rep.* **2013**, *3*, 3314.
- [9] S. Liu, Z. Chen, N. Zhang, Z.-R. Tang, Y. J. Xu, *J. Phys. Chem. C* **2013**, *117*, 8251.
- [10] a) Y. Xu, Z.-C. Fu, S. Cao, Y. Chen, W.-F. Fu, *Catal. Sci. Technol.* **2017**, Advance Article, <https://doi.org/10.1039/C6CY01568A>. b) X. Dai, M. Xie, S. Meng, X. Fu, S. Chen, *Appl. Catal. B* **2014**, *158*, 382.
- [11] N. Zhang, M.-Q. Yang, Z.-R. Tang, Y.-J. Xu, *ACS Nano* **2014**, *8*, 623.
- [12] a) W. Wu, G. Liu, Q. Xie, S. Liang, H. Zheng, R. Yuan, W. Su, L. Wu, *Green Chem.* **2012**, *14*, 1705. b) X. Ning, S. Meng, X. Fu, X. Ye, S. Chen, *Green Chem.* **2016**, *18*, 3628. c) S. K. Pahari, P. Pal, D. N. Srivastava, S. C. Ghosh, A. B. Panda, *Chem. Commun.* **2015**, *51*, 10322.
- [13] a) L. Crespo, G. Sanclimens, M. Pons, E. Giral, M. Royo, F. Albericio, *Chem. Rev.* **2005**, *105*, 1663. b) V. R. Pattabiraman, J. W. Bode, *Nature* **2011**, *480*, 471. c) A. El-Faham, F. Albericio, *Chem. Rev.* **2011**, *111*, 6557. d) C. L. Allen, J. M. Williams, *J. Chem. Soc. Rev.* **2011**, *40*, 3405.
- [14] R. M. Lanigan, T. D. Sheppard, *Eur. J. Org. Chem.* **2013**, 7453.
- [15] J. E. Anderson, R. Davis, R. N. Fitzgerald, J. M. Haberman, *Synth. Commun.* **2006**, *36*, 2129.
- [16] a) T. Marcelli, *Angew. Chem. Int. Ed.* **2010**, *49*, 6840. b) K. Ishihara, *Tetrahedron* **2009**, *65*, 1085. c) K. Ishihara, S. Ohara, H. Yamamoto, *J. Org. Chem.* **1996**, *61*, 4196. d) P. Tang, *Org. Synth.* **2005**, *81*, 262. e) R. M. Al-Zoubi, O. Marion, D. G. Hall, *Angew. Chem. Int. Ed.* **2008**, *47*, 2876. f) H. Charville, D. Jackson, G. Hodges, A. Whiting, *Chem. Commun.* **2010**, *46*, 1813. g) T. M. E. Dine, W. Erb, Y. Berhault, J. Rouden, J. Blanchet, *J. Org. Chem.* **2015**, *80*, 4532. h) R. M. de Figueiredo, J.-S. Suppo, J.-M. Campagne, *Chem. Rev.* **2016**, *116*, 12029. i) T. B. Halima, J. K. Vandavasi, M. Shkooor, S. G. Newman, *ACS Catal.* **2017**, *7*, 2176.
- [17] a) C. M. Gabriel, M. Keener, F. Gallou, B. H. Lipshutz, *Org. Lett.* **2015**, *17*, 3968. b) D. S. MacMillan, J. Murray, H. F. Sneddon, C. Jamieson, A. J. B. Watson, *Green Chem.* **2013**, *15*, 596. c) Q. Wang, Y. Wang, M. Kurosu, *Org. Lett.* **2012**, *14*, 3372. d) K. Hojo, A. Hara, H. Kitai, M. Onishi, H. Ichikawa, Y. Fukumori, K. Kawasaki, *Chem. Cent. J.* **2011**, *5*, 49. e) A. S. Galanis, F. Albericio, M. Grötl, *Org. Lett.* **2009**, *11*, 4488. f) S. M. A. Salam,

- K. Kagawa, K. Kawashiro, *Tetrahedron: Asymmetry* **2006**, *17*, 22. g) M. Kunishima, H. Imada, K. Kikuchi, K. Hioki, J. Nishida, S. Tani, *Angew. Chem., Int. Ed.* **2005**, *44*, 7254. h) R. De Marco, A. Tolomelli, A. Greco, L. Gentilucci, *ACS Sustainable Chem. Eng.* **2013**, *1*, 566.
- [18] N. Shangguan, S. Katukojvala, R. Greenberg, L. J. Williams, *J. Am. Chem. Soc.* **2003**, *125*, 7754.
- [19] Y. Rao, X. Li, S. J. Danishefsky, *J. Am. Chem. Soc.* **2009**, *131*, 12924.
- [20] a) D. Crich, K. Sasaki, *Org. Lett.* **2009**, *11*, 3514. b) Y. Rao, X. Li, S. J. Danishefsky, *J. Am. Chem. Soc.* **2009**, *131*, 12924. c) X. Wu, J. L. Stockdill, P. K. Park, S. J. Danishefsky, *J. Am. Chem. Soc.* **2012**, *134*, 2378.
- [21] F. B. Dyer, C. M. Park, R. Joseph, P. Garner, *J. Am. Chem. Soc.* **2011**, *133*, 20033.
- [22] D. Crich, K. Sana, S. Guo, *Org. Lett.* **2007**, *9*, 4423.
- [23] J. Pan, N. O. Devarie-Baez, M. Xian, *Org. Lett.* **2011**, *13*, 1092.
- [24] D. Crich, I. Sharma, *Angew. Chem., Int. Ed.* **2009**, *48*, 2355.
- [25] W. T. Wu, Z. H. Zhang, L. S. Liebeskind, *J. Am. Chem. Soc.* **2011**, *133*, 14256.
- [26] a) S. M. Mali, S. V. Jadhav, H. N. Gopi, *Chem. Commun.* **2012**, *48*, 7085. b) S. M. Mali, R. D. Bhaisare, H. N. Gopi, *J. Org. Chem.* **2013**, *78*, 5550.
- [27] H. Liu, L. Zhao, Y. Yuan, Z. Xu, K. Chen, S. Qiu, H. Tan, *ACS Catal.* **2016**, *6*, 1732.
- [28] E. L. Tyson, M. S. Ament, T. P. Yoon, *J. Org. Chem.* **2013**, *78*, 2046.
- [29] S. Das, S. Samanta, S. K. Maji, P. K. Samanta, A. K. Dutta, D. N. Srivastava, B. Adhikary, P. Biswas, *Tetrahedron Lett.* **2013**, *54*, 1090.
- [30] W. Wang, W. Feng, T. Ding, Q. Yang, *Chem. Mater.* **2015**, *27*, 6181.
- [31] D.-S. Kong, *Langmuir* **2008**, *24*, 5324.
- [32] X. Yang, A. Wolcott, G. Wang, A. Sobo, R. C. Fitzmorris, F. Qian, J. Zhang, Y. Li, *Nano Lett.* **2009**, *9*, 2331.
- [33] a) R. H. Liu, L. E. Orgel, *Nature* **1997**, *389*, 52. b) P. Wang, X. C. Li, J. L. Zhu, J. Chen, Y. Yuan, X. Y. Wu, S. J. Danishefsky, *J. Am. Chem. Soc.* **2011**, *133*, 1597.
- [34] a) K. P. Acharya, R. S. Khnayzer, T. O. Connor, G. Diederich, M. Kirsanova, A. Klinkova, D. Roth, E. Kinder, M. Imboden, M. Zamkov, *Nano Lett.* **2011**, *11*, 2919. b) J. D. Gough, J. M. Gargano, A. E. Donofrio, W. J. Lees, *Biochemistry* **2003**, *42*, 11787. c) T. V. DeCollo, W. J. Lees, *J. Org. Chem.* **2001**, *66*, 4244. d) P. Schapotschnikow, B. Hommersom, T. J. H. Vlugt, *J. Phys. Chem. C* **2009**, *113*, 12690. e) J. Aldana, N. Lavelle, Y. Wang, X. Peng, *J. Am. Chem. Soc.* **2005**, *127*, 2496.
- [35] R. Zhao, J. Lind, G. Merényi, T. E. Eriksen, *J. Am. Chem. Soc.* **1998**, *120*, 2811.
- [36] R. Zhao, J. Lind, G. Merényi, T. E. Eriksen, *J. Phys. Chem. A* **1999**, *103*, 71.
- [37] a) J. A. Imlay, *Annu. Rev. Microbiol.* **2003**, *57*, 395. b) F. Su, S. C. Mathew, G. Lipner, X. Fu, M. Antonietti, S. Blechert, X. Wang, *J. Am. Chem. Soc.* **2010**, *132*, 16299.

SUPPORTING INFORMATION

Additional Supporting Information may be found online in the supporting information tab for this article.

Data and ^1H spectra of compounds **3aa** to **3bc**.

How to cite this article: Das S, Ray S, Ghosh AB, et al. Visible light driven amide synthesis in water at room temperature from Thioacid and amine using CdS nanoparticles as heterogeneous Photocatalyst. *Appl Organometal Chem.* 2017; e4199. <https://doi.org/10.1002/aoc.4199>